Local fat content determines global and local stiffness in fatty livers

[Fat accumulation locally softens liver]

David Li[1,2], Paul A. Janmey[2,3,4,5], and Rebecca G. Wells[1,2,3]

[1]Division of Gastroenterology and Hepatology, Department of Medicine
[2]NSF Science and Technology Center for Engineering MechanoBiology
[3]Department of Bioengineering
[4]Institute for Medicine and Engineering
[5]Department of Physiology
University of Pennsylvania, Philadelphia, PA

Grant Support:
This work was supported by NIH grant R01EB017753 to PAJ and RGW and by the Center for Engineering MechanoBiology (CEMB), an NSF Science and Technology Center, under grant agreement CMMI1548571.

Abbreviations:
NAFLD, non-alcoholic fatty liver disease; NASH, non-alcoholic steatohepatitis; DAPI, 4',6'-diamidino-2-phenylindole

Correspondence:
Rebecca G. Wells
905 BRB II/III
421 Curie Boulevard
Philadelphia, PA 19104-6140
Email: rgwells@pennmedicine.upenn.edu
Tel.: +1-215-573-1860

Disclosures:
The authors disclose no conflicts.

Data Transparency:
All study data are included in the article and/or supplementary material, and all analytic methods are available upon request from the authors.

Abstract

Nonalcoholic fatty liver disease (NAFLD) refers to a spectrum of pathology characterized by steatosis and other changes to the liver not associated with heavy alcohol use. NAFLD is the most common form of liver disease globally, affecting over 80 million people in the United States. The contribution of mechanical changes resulting from fat accumulation to NAFLD progression is unclear and the effect of steatosis on the mechanical properties of the liver has yet to be defined. We studied the livers of ob/ob and wild-type littermate mice using parallel plate rheometry as well as a sub-millimeter scale microindentation technique to define the stiffness of steatotic livers. The microindentation technique was adapted to enable determination of local fat content and identification of other local features in the indented region. We found that steatotic livers and steatotic regions of fatty livers were softer than non-steatotic livers/regions. Higher lipid content in a region correlated with decreased stiffness. The finding that steatosis is associated with both global and local liver softening has significant implications for understanding the progression of early stage NAFLD, given that stiffening is a mechanical stimulus for the development of fibrosis.

Manuscript

Nonalcoholic fatty liver disease (NAFLD) refers to a spectrum of pathology characterized by liver steatosis and other changes to the liver not associated with heavy alcohol use.[1] NAFLD is the most common form of liver disease globally, affecting over 80 million people in the United States.[1,2] In NAFLD, simple steatosis can progress to non-alcoholic steatohepatitis (NASH), fibrosis, cirrhosis and end-stage liver disease, and hepatocellular carcinoma.[3] Inflammation, as in NASH, promotes fibrosis.[4] However, NAFLD progression is mechanistically complex and poorly understood.[4]

The contribution of mechanical changes resulting from fat accumulation to NAFLD progression is unclear. Liver stiffening precedes fibrosis in rodent models of liver injury and promotes hepatic stellate cell myofibroblast differentiation and fibrogenesis.[5,6] The effect of steatosis itself on the mechanical properties of the liver has yet to be defined. Clinical elastography methods to determine liver stiffness reflect confounding factors such as venous pressure and have yielded contradictory results,[7] while previous ex vivo rheology studies have focused on stiffening associated with fibrosis.[8]

To determine the effect of fat accumulation on the mechanical properties of the liver as a whole, we compared steatotic and non-steatotic mouse livers ex vivo by parallel plate rheometry. We used ob/ob mice as a model of liver steatosis without fibrosis, with wild-type littermates as controls. Livers

were removed at 8, 12, and 36 weeks of age, and H&E staining demonstrated an increase in lipid droplets in ob/ob mice at all ages compared to controls (Figure 1A). Picrosirius red staining confirmed the absence of fibrosis in both ob/ob and control livers (Figure 1B and Supplementary Figure 1). Shear rheometry was performed on liver cores[5] to determine the shear storage modulus G', the shear loss modulus G", and Young's modulus E, showing that livers from ob/ob mice were significantly softer and had less pronounced compression stiffening than those from age-matched controls (Figure 1C). Thus, steatosis results in overall liver softening.

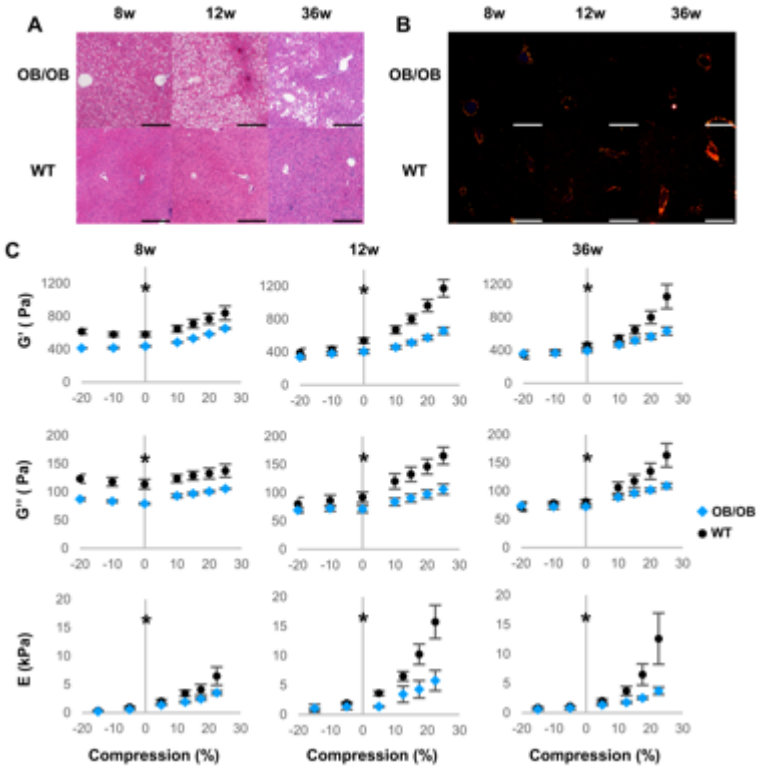

Figure 1. Simple steatosis induces liver softening in ob/ob mice. (A) Representative H&E stains of livers from ob/ob mice and wild type littermates at 8w, 12w, and 36w of age. (B) Representative picrosirius red stains of ob/ob and wt livers taken under polarized light microscopy. Scale bar = 250 μm. (C) Shear elastic modulus G', shear loss modulus G", and Young's modulus E of ob/ob (blue) and wt (black) livers at 8w, 12w, and 36w under varied tension and compression. Under all metrics, ob/ob livers were significantly softer than wt livers. $n \geq 4$ animals for each condition. Error bars indicate standard error. * $P < 0.005$ by two-way ANOVA.

Fat accumulation is heterogeneous in NAFLD, preferentially localizing to regions around the central veins.[9] We therefore next asked whether localized lipid accumulation induces localized softening.

To measure regions of fat accumulation at the submillimeter scale, we adapted a previously described microindentation technique[10] in order to both measure stiffness and examine cell structures such as lipid droplets within the same submillimeter regions of the liver (Figure 2A). 4',6'-diamidino-2-phenylindole (DAPI) was applied to liver cores after maximal indentation, staining around but not under the indenter and resulting in a ring demarcating the region where stiffness was measured. After release of the indenter, whole mount Oil Red O staining was used to label lipids. Finally, epifluorescence microscopy was performed to capture demarcation, lipid accumulation, and autofluorescence of the liver, the latter of which was used to avoid large vasculature structures (Figure 2B and Supplementary Figure 2).

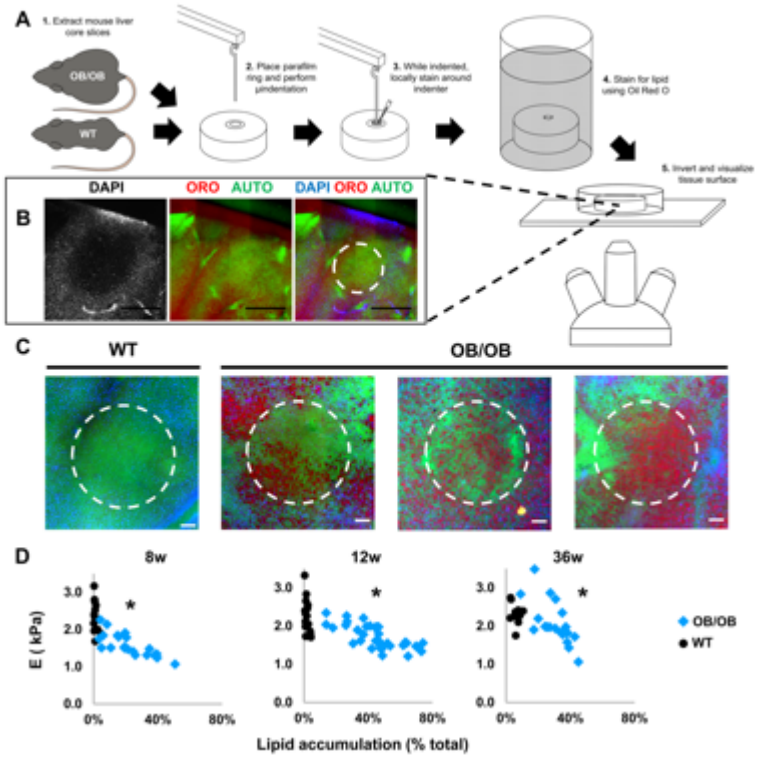

Figure 2. Increased local lipid accumulation in steatosis is associated with local softening. (A) Schematic of technique combining demarcation of microindented regions with visualization of tissue features. (B) Whole mount epifluorescence microscopy images of a 12w wt liver showing DAPI (blue) demarcating the microindented region (left), autofluorescence (green) and heterogeneous lipid accumulation using Oil Red O (red, middle), and the three channels merged (right) showing low lipid within the indented region (white dashed line). Scale bar 500 μm. (C) Representative fluorescent images of indented wt and ob/ob livers with increasing lipid accumulation within the indented region. Scale bar 100 μm. (D) Scatter plots of Young's Modulus E vs. lipid accumulation within microindented regions of ob/ob (blue) and wt (black) livers taken at 8w, 12w, and 36w. Submillimeter regions of ob/ob livers with greater local steatosis had lower local stiffness at all tested ages. $n \geq 11$ measurements from ≥ 3 animals for each condition. * $r_s < -0.7$ and $P < 0.005$ by Spearman's rank correlation.

The amount of fat within the demarcated regions was greater in ob/ob livers than controls, and there was significant variation in different demarcated regions in ob/ob livers (Figure 2C). To examine the relationship between local stiffness and local fat accumulation, we quantified the amount of lipid staining in the demarcated microindented regions and found a significant inverse correlation between fat content and local stiffness through Spearman's rank correlation, indicating that local fat accumulation of simple steatosis results in associated local softening (Figure 2D). The 12w samples, which had the highest lipid accumulation, demonstrated a plateau (percolation threshold) at approximately 50-60% lipid, beyond which there was no further softening observed.

The finding that steatosis is associated with both global and local liver softening has significant implications for understanding the progression of early stage NAFLD, given that stiffening is a mechanical stimulus for the development of fibrosis. In the absence of bulk stiffening, locally soft areas are in particular contrast to other features of the liver microarchitecture, such as vasculature. Uncovering the relationship between these microscale mechanical features may yield mechanistic insights into the progression of NAFLD. The ability to correlate submillimeter-scale stiffness measurements with histological features can also be used to study other pathological states, such as steatohepatitis and fibrosis, and to investigate development and disease in other tissues and organ systems.

Acknowledgements

The authors thank Jessica Llewellyn, Dongning Chen, Xuechen Shi, and Jeff Byfield for training, technical support, and feedback, the Center for Molecular Studies in Digestive and Liver Diseases (P30DK050306) for histology and microscopy support, Guy Genin for thought-provoking discussions, and Yang Liu for assistance with the illustration.

131 **References**

132 1. Chalasani N, et al. *Hepatology*. 2018; **67**: 328-357

133 2. Estes C, et al. *Hepatology*. 2018; **67**: 123-133

134 3. Matteoni CA, et al. *Gastroenterology*. 1999; **116**: 1413-1419

135 4. Friedman SL, et al. *Nat Med*. 2018; **24**: 908-922

136 5. Perelpelyuk M, et al. *Am J Physiol Gastrointest Liver Physiol*. 2013; **304**: G605-G614

137 6. Olsen AL, et al. *Am J Physiol Gastrointest Liver Physiol*. 2011; **301**: G110-G118

138 7. Mueller S, et al. *World J Gastroenterol*. 2010; **16**: 966-972

139 8. Chin L, et al. Am J Physiol Gastrointest Liver Physiol. 2020; **319**: G11-G22

140 9. Takahashi Y, et al. *World J Gastroenterol*. 2014; **20**: 15539-15548

141 10. Levental I, et al. *J Phys Condens Matter*. 2010; **22**: 194120-194120

142

143 **Supplementary information**

144 **Steatotic livers soften with local stiffness determined by local fat content**
145
146 [Fat accumulation locally softens liver]
147
148 *David Li[1,2], Paul A. Janmey[2,3,4,5,6], and Rebecca G. Wells[1,2,3,4]*
149

150 **Materials and Methods**

151 *Animal studies*

152 All animal work was carried out in strict accordance with the recommendations in the Guide for
153 the Care and Use of Laboratory Animals of the National Institutes of Health. Animal protocols were
154 approved by the Institutional Animal Care and Use Committee of the University of Pennsylvania
155 (protocol #804031). Ob/ob mice were obtained from the Jackson Laboratories (strain #000632). Animals
156 were housed in a temperature-controlled environment with appropriate enrichment, ad libitum feeding of
157 standard rodent chow and water, and 12h light/dark cycles. Euthanasia was carried out by CO_2
158 inhalation followed by exsanguination. Livers were harvested from ob/ob mice and wild type littermates
159 at 8w, 12w, and 36w and stored in PBS at 4°C for up to 5h before being analyzed; rodent livers are
160 adequately preserved under these conditions and rheological properties are maintained.[1,2]

161 *Shear rheometry*

162 Shear rheometry was performed as described previously.[1] Briefly, liver samples were prepared
163 using an 8 mm punch (MP0144, Alabama R&D) with all punches taken in the same orientation from the
164 same lobe. The height of the slices ranged from 2.0 to 3.9 mm in the uncompressed state. Samples were
165 kept hydrated during all experiments with PBS. Parallel plate shear rheometry was carried out on a
166 Kinexus PRO rheometer (Kinexus series, Malvern Instruments) at room temperature. Samples were
167 attached to rheometer platforms with fibrin glue by applying 5 μL each of 20 mg/mL bovine plasma
168 fibrinogen (341573, Sigma-Aldrich) and 100 U/mL bovine thrombin (T4648, Sigma-Aldrich) to both the
169 top and bottom side of the sample. The upper platen was quickly lowered until 0.02 N of nominal initial

force was applied to ensure adhesive contact of the sample with the metal surfaces of the rheometer, and the sample was allowed to sit for 10 min for the fibrin glue to polymerize fully before performing measurements. Previous literature indicates that the fibrin glue does not affect the mechanics of the system.[1] Mechanics were measured with a dynamic time sweep test (2% constant strain, oscillation frequency 1rad/s, measurements taken for 120s). These measurements were carried out under the uncompressed condition, then increasing uniaxial tension (10% and 20%), then the uncompressed condition followed by increasing uniaxial compression (10, 15, 20, and 25%). Tension and compression were applied by changing the gap between the platform and upper platen of the rheometer. The following correction was applied to account for the change in cross-sectional area during testing under the assumption that total tissue volume is conserved, where G' is the storage modulus and λ is axial strain:

$$G'_{actual} = G'_{measured}(1+\lambda)^2$$

A similar correction was applied to the loss modulus G'' and normal stress δ, and Young's modulus E was determined by calculating the slope of stress (Pa) vs axial strain[1].

Microindentation and demarcation of microindented regions

Microindentation was performed as described previously[3], with additional modifications to permit the demarcation and visualization of mesoscale features within the microindented region of the tissue. Briefly, the microindentation device consists of a stepping motor (L4018S1204-M6, Nanotec) attached to a μN-resolution tensiometric probe adapted from the surface tension measurement apparatus of a Langmuir monolayer trough (MicroTrough X, Kibron Inc), consisting of a 0.510 mm diameter blunt-ended cylindrical tungsten alloy wire hung from a digital microbalance. The force-displacement relationship was found to behave as a Hookean spring (force linearly related to displacement - k_{probe} ~ 4.5N/m) with the spring constant calibrated prior to each measurement.

Liver samples 3 mm thick were prepared from liver tissue cores obtained using an 8 mm punch, removing the Glisson's capsule. A ring of Parafilm was prepared using a 2 mm disposable biopsy punch

195 and placed on top of the liver sample. Samples were then manually positioned under the free-hanging
196 probe, followed by downward displacement of the probe until contact occurred between the probe and
197 the sample in the center of the Parafilm ring. Following establishment of contact between probe and
198 sample, the probe was translated downward at a continuous rate of 0.0125 mm/s. These translations
199 resulted in decreases in measurable force from the probe, which were converted into local Young's
200 modulus as described previously.[3] After the probe was fully indented into the sample (as determined by
201 no measurable force from the probe), 0.5 μL of 100 μg/mL DAPI (D1306, Invitrogen) solution was
202 pipetted around the probe and allowed to selectively stain within the Parafilm ring for 15s before
203 washing with PBS. Multiple measurements were obtained per liver sample using this approach. After
204 microindentation and demarcation, liver samples were stored in PBS at 4°C for up to 5h before being
205 stained and imaged for lipid accumulation.

206 *Visualization and quantification of lipid accumulation of microindented regions*

207 Liver samples were stained for lipid using an adaptation of whole mount Oil Red O staining.[4] All
208 incubation steps were performed at room temperature on a shaker. Briefly, samples were incubated with
209 0.5% Tween 20 (#170-6531, Bio-Rad) in PBS for 15min, changing the solution every 5min, before
210 incubating with 0.5% Oil Red O in propylene glycol (D1306, Poly Scientific R&D Corp) for 15min.
211 Afterwards, the samples were washed once with Tween solution before incubating with Tween solution
212 for 15min, changing the solution every 5min.

213 Visualization of lipid accumulation within microindented regions was performed using whole
214 mount epifluorescence microscopy on a Nikon Eclipse Ti widefield microscope equipped with a 4x/0.31
215 N.A. PlanFluor dry objective lens and motorized stage. Lipid[5], DAPI demarcation, and liver
216 autofluorescence were visualized using Cy3, DAPI, and FITC filters respectively. Quantification of lipid
217 accumulation within demarcated DAPI rings was performed by thresholding the Cy3 channel in ImageJ.

218 *Statistical analysis*

Statistical significance of differences between strain-dependent shear rheometry curves (G', G'', and E) of ob/ob mice and wild type mice were determined using two-way ANOVA.[1] Statistical significance of the decreasing monotonic trend between increasing local lipid accumulation and local stiffness within sub-mm regions of the ob/ob and wild type mouse liver was determined using Spearman's rank correlation coefficient.[6] For all statistical analyses, a P value of ≤ 0.05 was considered significant.

Supplementary Figures

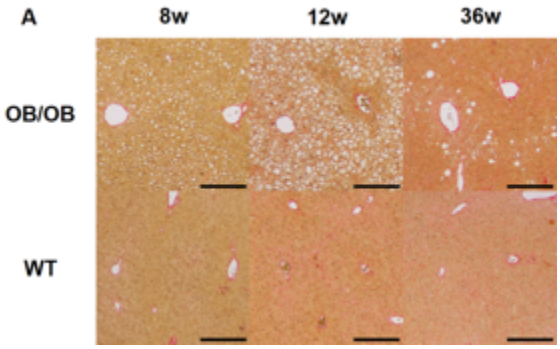

Supplementary Figure 1: Ob/ob mice do not show fibrosis. Representative picrosirius red stains of ob/ob and wt livers taken at 8w, 12w, and 36w under brightfield microscopy. Images are of the same regions from Figure 1B. Scale bars = 250 μm.

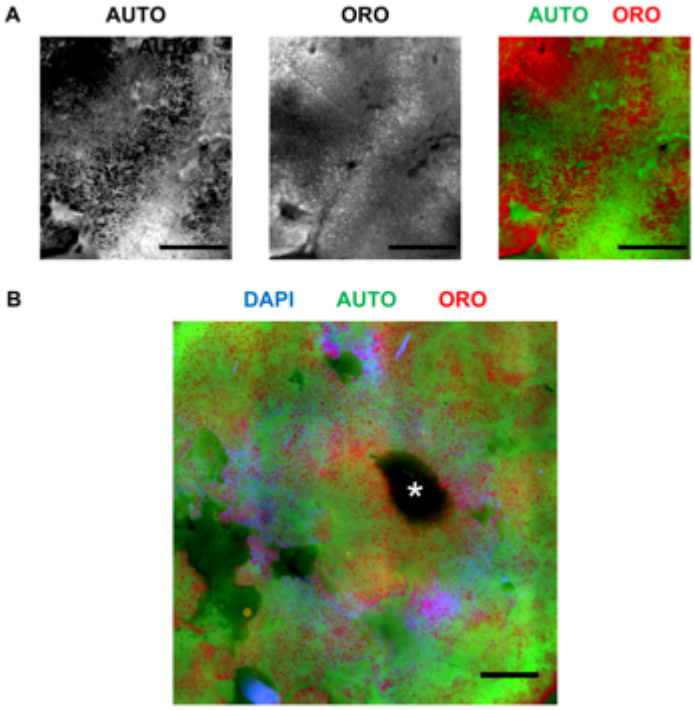

Supplementary Figure 2: Whole mount fluorescent staining and microscopy shows submillimeter features within ob/ob livers. (A) Representative fluorescent images of autofluorescence (left) and intracellular lipid accumulation within hepatocytes show spatial heterogeneity of lipid accumulation at the submillimeter scale within 12w ob/ob livers. (B) Epifluorescent composite image of a 12w ob/ob liver with region of indentation from a 1 mm indenter marked with DAPI and stained for lipid accumulation (Dapi, blue; autofluorescence, green; lipid, red). * indicates an intrahepatic blood vessel within the indented region. Scale bars = 500 μm.

References

1. Perepelyuk M, et al. *PLoS One.* 2016; **11**: e0146588.
2. Tan K, et al. *J Biomech.* 2013; **46**: 1060-1066.
3. Levental I, et al. *J Phys Condens Matter.* 2010; **22**: 194120.
4. Kim S-H, et al. *PLoS One.* 2015; **10**: e0125980.
5. Koopman R, et al. *Histochem Cell Biol.* 2001; **116**: 63-68.
6. Sünderhauf A, et al. *Cell Mol Gastroenterol Hepatol.* 2021; **12**: 229-250.